ELSEVIER

International Journal of Solids and Structures 41 (2004) 1119–1137

INTERNATIONAL JOURNAL OF SOLIDS and STRUCTURES

www.elsevier.com/locate/ijsolstr

A class of expandable polyhedral structures

F. Kovács [a], T. Tarnai [b,*], P.W. Fowler [c], S.D. Guest [d]

[a] *Research Group for Computational Structural Mechanics, Hungarian Academy of Sciences, Műegyetem rkp. 3, Budapest H-1521, Hungary*

[b] *Department of Structural Mechanics, Budapest University of Technology and Economics, Műegyetem rkp. 3, Budapest H-1521, Hungary*

[c] *School of Chemistry, University of Exeter, Stocker Road, Exeter EX4 4QD, UK*

[d] *Department of Engineering, University of Cambridge, Trumpington Street, Cambridge CB2 1PZ, UK*

Received 4 October 2002; received in revised form 9 June 2003

Abstract

A class of expandable polyhedral structures, the expandohedra, consisting of prismatic faces linked along edges by hinged plates, provides a model for the swelling of viruses. The finite breathing mode of the expandohedra, apparent in the model, and from geometric arguments, is not, however, detected by elementary counting techniques. Symmetry extended mobility criteria show that the breathing motion is part of a set of face mechanisms for many expandohedra. Numerical analysis using the singular value decomposition of the compatibility matrix confirms the completeness of the deductions from general symmetry theorems, derived for expandohedra.

Keywords: Symmetry; Group theory; Regular polyhedra; Mechanism; Deployable/retractable structures; Mobility criteria

1. Introduction

Certain viruses having the shape of a truncated icosahedron expand under the effect of pH change in biological media (Speir et al., 1995). The pentamers and hexamers move apart from each other, rotating but remaining in contact through protein links. The discovery of this phenomenon calls attention to the problem of motion of expandable polyhedra.

The characteristics of the virus motion differ from those of another expanding object, the popular toy known as the Hoberman Sphere™ (Hoberman, 1991). This *transforming globe* defines an underlying polyhedron, whose faces preserve their orientation as they expand. In the virus, however, the faces essentially preserve their size but each is subjected to a translation and rotation along its symmetry axes and, as the virus expands, interstices appear between the faces. Thus, the swelling motion of the virus, although complex and still incompletely understood, seems to be more similar to a special type of deformation that

* Corresponding author. Tel.: +36-1-463-1431; fax: +36-1-463-1099.
E-mail address: tarnai@ep-mech.me.bme.hu (T. Tarnai).

0020-7683/$ - see front matter © 2003 Elsevier Ltd. All rights reserved.
doi:10.1016/j.ijsolstr.2003.09.046

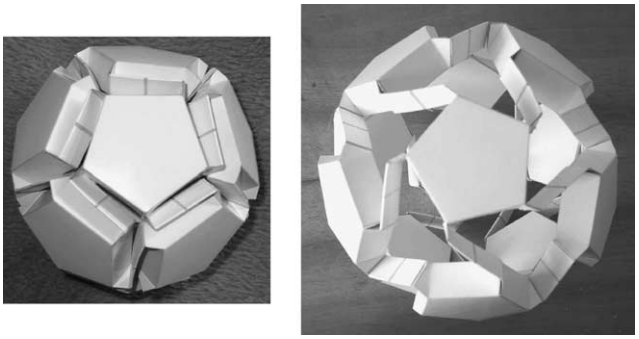

Fig. 1. A cardboard model of an expandable dodecahedron, shown in closed and partially open configurations.

has been studied for honeycombs (Kollár and Hegedűs, 1985), and to the motion exhibited by Fuller's (1975) *jitterbug*.

In order to gain a better insight into the virus problem, Kovács and Tarnai (2000) initiated a study of the motion of a simpler object: an expandable dodecahedron (Fig. 1). A physical model exhibited the breathing expansion mode that was expected on intuitive grounds, although paradoxically it turns out that this mode is not accounted for by mobility analysis using standard techniques.

The expandable dodecahedron suggests a class of similar objects, the *expandohedra*, which will also be studied in this paper. These expandable polyhedra have analogues in fullerene chemistry; they model the *leapfrog* transformation (Fowler and Steer, 1987), which produces fullerenes with ideal π-electronic structures. A fullerene, and in fact any convex polyhedron, can be converted into its leapfrog by a two-stage procedure. If an original fullerene polyhedron is capped on every face, a deltahedron is obtained, and if this deltahedron is then converted to its dual, a new fullerene polyhedron with three times as many vertices is obtained. Leapfrogging is a discontinuous process which jumps from one fullerene to another over the intervening deltahedron. For example, the leapfrog transformation converts a dodecahedron to a truncated icosahedron. It turns out that this particular transformation can alternatively be described as a continuous process using Verheyen's (1989) dipolygonid composed of 30 digons and 12 pentagons, which he denotes by the symbol $30\{2\} + 12\{5\}|31.717474°$. The expandohedra provide an alternative continuous description for this, and for certain other, leapfrog transformations.

The expandohedron can also be considered as a *deployable structure* providing a large volume expansion. The fully open expandohedron has a number of mechanisms, see below, but the addition of e.g. locking hinges (Seffen et al., 1999) would give rigidity to the deployed structure.

This paper has therefore two aims. The first is to provide a detailed analysis of the mobility of the expandable dodecahedron, and the second is to place the dodecahedron within a general class of expandable polyhedra, providing general symmetry theorems for their mobility. The paper brings together a number of different techniques to analyse the kinematics of these novel deployable systems. New features arise at each level of analysis. Section 2 contains a geometric analysis of the finite breathing motion in a particular case, the expanding dodecahedron, and identifies by geometric arguments additional sets of possible infinitesimal motions. Section 3 uses recently developed symmetry techniques (Kangwai and Guest, 1999, 2000; Fowler and Guest, 2000) to find and classify the possible motions of several general classes of expandohedra; the finite breathing mode is shown to be symmetrically distinct from the mechanisms that can be found by simple counting. Section 4 reports the results of detailed numerical analysis of open and closed configurations of particular expandohedra, giving a complete account of the kinematics, and confirming the results of the more general symmetry analysis. This combination of techniques proves to be an effective route to understanding the behaviour of complex kinematic systems.

2. A physical model of the expandable dodecahedron

2.1. Structure

The expandable polyhedral viruses have the basic property that all pentamers and hexamers are situated in icosahedral symmetry at any stage of swelling. To simulate the expansion of these viruses, a dodecahedral assembly producing this symmetrical motion was constructed. The cardboard model in Fig. 1 represents a mechanism composed of rigid bodies with hinged connections.

The dodecahedron cardboard model was designed under the following constraints:

(i) the structure consists entirely of equal rigid bodies (pentagonal prisms) and rigid connecting elements (triangular and rectangular plates);
(ii) all connections between prism and plate, and between plate and plate, are revolute hinges;
(iii) the whole assembly must have icosahedral rotational symmetry I. As a consequence, all chains of connecting elements between adjacent pentagonal prisms are identical and must have a two-fold rotational symmetry C_2;
(iv) all conditions of compatibility should be satisfied in any position during the expansion motion.

In this particular model, regular pentagon-based straight prisms were used, and triangles and rectangles were used as planar connecting elements. In Fig. 2, two adjacent pentagonal prisms are shown with their mode of connection. In what follows, the pentagonal prisms will usually be referred to as pentagons, except when the third dimension of the prism is relevant to the geometrical description.

2.2. Type and range of expansion

A clearly detectable motion of the structure, as built according to the requirements listed above, is a symmetrical expansion. In this motion, each pentagonal prism rotates about its axis of five-fold symmetry by the same angle, and simultaneously moves along this axis radially outwards with the same speed, that is, the pentagons are at equal distance from the centre. Consequently, in any position, the plane of a pentagon is parallel to that of the same pentagon in the initial position. In other words, all inclination angles between adjacent pentagonal prisms remain constant. Let this angle be denoted by ϕ. If edges BC and DE in Fig. 2 are parallel to the bisector of ϕ, then $\angle ABC$ and $\angle DEF$ are equal to $\phi/2$. Since the initial configuration is the regular dodecahedron, ϕ is identical to the angle subtended by an edge of a regular icosahedron on the unit sphere.

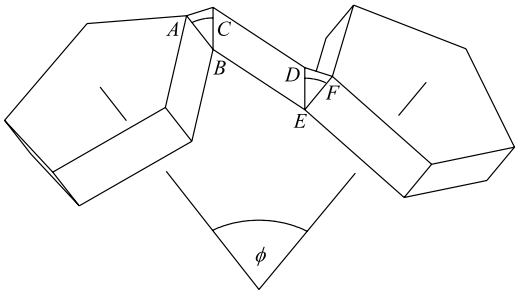

Fig. 2. Two pentagonal prisms and their connection.

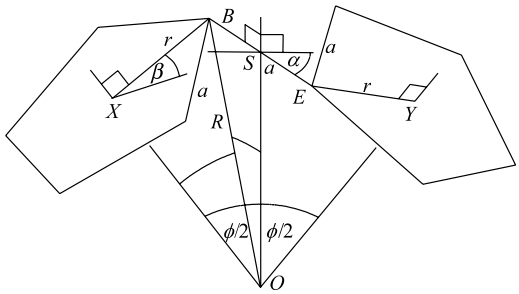

Fig. 3. Simplified network of two pentagonal prisms (showing inner edges and vertices only).

Let the edge length of a regular pentagon be equal to the side BE of the connecting rectangle in Fig. 2, and let this common length be denoted by a. Additionally, let the circumradius of the pentagon be r. Consider now the network determined by the inner vertices of the pentagonal prisms, and consider two adjacent pentagons of centre X and Y (Fig. 3). This is a part of the dipolygonid mentioned earlier. By the requirement of icosahedral symmetry, the vertices of the pentagons should lie on a sphere of radius R and centre O, and the adjacent pentagons of centre X and Y should be oriented in accordance with C_2 symmetry. Hence, the C_2 axis OS bisects the segment (i.e. the digon) BE perpendicularly. Since the pentagon of centre X translates along, and rotates about, the axis OX, the vertices of this pentagon move on the surface of a right circular cylinder of radius r and axis OX; and similarly, since the segment (digon) connecting the two pentagons translates along, and rotates about, the axis OS, its end-points B and E move on the surface of a right circular cylinder of radius $a/2$ and axis OS. Therefore, compatibility is fulfilled if point E lies on the line of intersection of these two cylinders. Points of this line of intersection determine a relationship between the angle α of rotation of the connecting segment and the radius R of the circumscribed sphere. Thus, the motion of this assembly can be described as a function of one parameter. Compatibility is preserved if this assembly is supplemented in such a way that right prisms are placed on the pentagons, rectangles are placed on the connecting segments whose planes are passing through point O, and the gaps between the respective edges of the pentagonal prisms and rectangles are filled by triangles. By the above argument, the angles between the respective edges of the pentagonal prisms and rectangles do not change during the motion—planes ABC and DEF remain parallel to one another, and to their initial position. Therefore, as it supports this expansion–contraction breathing type of motion, the dodecahedron model is a finite mechanism.

In order to determine the relationship between α and R, first let us project the centres X, Y, Z of three mutually adjacent faces of a dodecahedron onto the unit sphere concentric with the dodecahedron (Fig. 4).

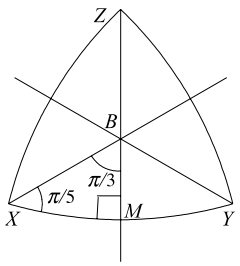

Fig. 4. A vertex (B) with three adjacent faces (centres X, Y, Z) shown in spherical projection.

The arc drawn from the vertex B to the mid-point M of arc XY is perpendicular to arc XY. The cosine rule for the angles of spherical triangle BMX shows that

$$\cos\angle XBM = -\cos\angle BMX\cos\angle MXB + \sin\angle BMX\sin\angle MXB\cos XM, \tag{1}$$

where $XM = \phi/2$, $\angle XBM = \pi/3$, $\angle BMX = \pi/2$, $\angle MXB = \pi/5$. Hence,

$$\cos\frac{\phi}{2} = \cos\frac{\pi}{3}/\sin\frac{\pi}{5} = \frac{1}{2}\csc\frac{\pi}{5}. \tag{2}$$

Now let us project the network of Fig. 3 onto the unit sphere of centre O, and denote the points in projection with the same letters as in the original. Then, the cosine rule for the sides of triangle XSB yields:

$$\cos BX = \cos XS\cos SB + \sin XS\sin SB\cos\angle XSB, \tag{3}$$

whence

$$\cos\angle XSB = \frac{\cos BX - \cos XS\cos SB}{\sin XS\sin SB}. \tag{4}$$

Here $\angle XSB = \alpha$, $XS = \phi/2$, $\sin SB = a/(2R)$, $\sin BX = \overline{BX}/\overline{BO} = r/R = a/(2R\sin(\pi/5))$. Substituting these expressions into (4), and taking into account (2) and the fact that $\sin(\pi/5) = \sqrt{(5-\sqrt{5})/8}$, we obtain:

$$\cos\alpha = \frac{2\sqrt{\frac{5-\sqrt{5}}{2}\left(\frac{R}{a}\right)^2 - 1} - \sqrt{\left(\frac{R}{a}\right)^2 - 1}}{\sqrt{\frac{3-\sqrt{5}}{2}}}, \tag{5}$$

and the inverse relation:

$$\frac{R}{a} = \frac{1}{2}\sqrt{(4+\sqrt{5})\cos^2\alpha + 2\cos\alpha\sqrt{(5+2\sqrt{5})\cos^2\alpha + 9 + 4\sqrt{5}} + (9+3\sqrt{5})/2}. \tag{6}$$

Since $\alpha = \pi/2$ results in the most compact (dodecahedral) configuration ($R = R_{\min}$) while $\alpha = 0$ in the fully expanded (truncated icosahedral) one ($R = R_{\max}$), we can calculate the minimum and maximum values of R/a: $R_{\min}/a = 1.401$; $R_{\max}/a = 2.478$. The ratio of these values shows that the circumradius of our model increases by about 77% during expansion. The volume of the dodecahedron is $a^3\sqrt{(235+105\sqrt{5})/8} = 7.663a^3$, and the same for the semi-regular truncated icosahedron is $a^3((3+\sqrt{5})45/4 - \sqrt{(15+5\sqrt{5})/2}) = 55.288a^3$. Thus, the volume of the fully expanded structure is 7.215 times larger than that of the dodecahedron.

To illustrate this expansion–contraction motion of the dodecahedron, we calculated the coordinates of the vertices of the pentagons as functions of angle α, and produced a series of snapshots of the expandable model for α varying from $\pi/2$ to 0 (Fig. 5).

Useful information can also be obtained by investigation of the coupled translation and rotation of a pentagon, that is, by determining the relationship between β and R, where β denotes the angle of rotation of a pentagon. Consider again the projection of the network in Fig. 3 on the unit sphere of centre O. Then, the sine rule for the spherical triangle BXS gives that

$$\frac{\sin\angle BXS}{\sin BS} = \frac{\sin\angle XSB}{\sin BX}. \tag{7}$$

Since $\angle XSB = \alpha$, $\angle BXS = \beta$, $\sin BS = a/(2R)$, $\sin BX = a/(2R\sin(\pi/5))$, from (7) we obtain:

$$\cos\alpha = \sqrt{1 - \left(\frac{\sin\beta}{\sin(\pi/5)}\right)^2}. \tag{8}$$

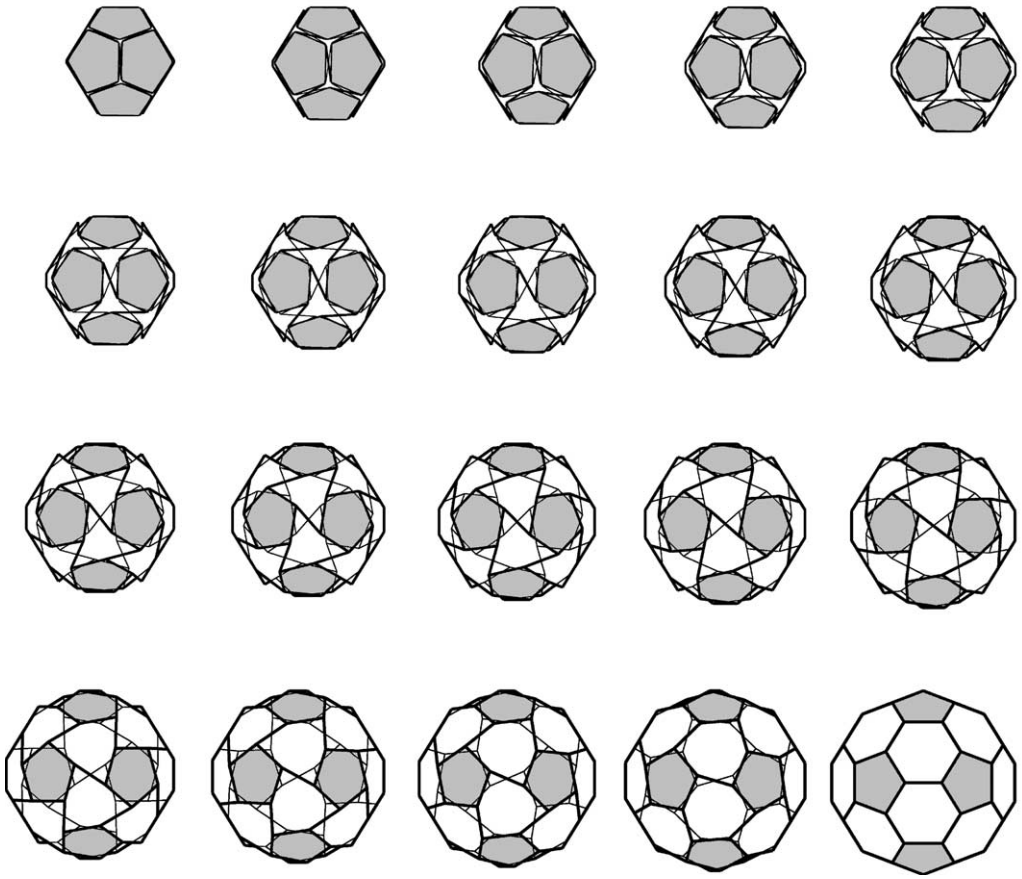

Fig. 5. Snapshots of the expansion process viewed down a C_2 axis of the dodecahedron.

The positive square root is taken, as this corresponds to the physically accessible configurations. Substituting (8) into (6) we can express R/a as a function of β. In Fig. 6, R/a is plotted versus β (the dashed line results from taking the negative square root in (8)). At $\beta = -\pi/5$, the configuration is closed (the dodecahedron); at $\beta = 0$ it is fully expanded (truncated icosahedron); at $\beta = \pi/5$ the configuration is closed again, but it is an enantiomorphic counterpart of the initial configuration (mirror image of the original). It is interesting to see that the curve in Fig. 6 has vertical tangents at points $\beta = \pm\pi/5$, as this means that the model can expand infinitesimally without rotation of the pentagons. The horizontal tangent at $\beta = 0$ shows that radius R has its maximum there, and at this point the pentagons can rotate infinitesimally without changing R.

2.3. Generalizations

The construction given for an expandable dodecahedron can be straightforwardly extended for all five Platonic polyhedra. All five of them have C_2 axes passing through edge midpoints, so hinged links composed of rigid rectangles and triangles which connect adjacent face prisms can be introduced. With appropriate changes to allow for the detailed geometry at the hinges, all the foregoing arguments for the expandable dodecahedral model apply to expandohedra based on the Platonic polyhedra. In particular, a

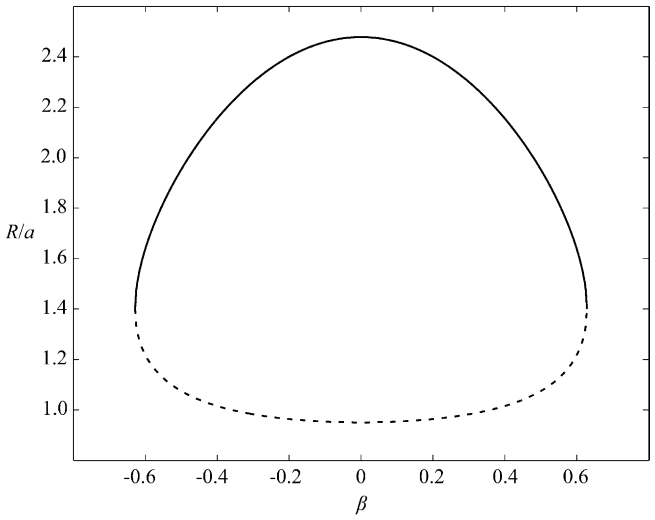

Fig. 6. Variation of the relative circumradius (R/a) with angle of rotation of the pentagons (β). The dashed line continues the solution of (8) into the non-physical regime where prisms would intersect.

finite expansion mechanism exists for all of them. In this way a whole class of expandable regular polyhedra (*expandohedra*) can be defined.

The expandohedra of particular interest are those whose parent polyhedra have trivalent vertices: tetrahedron, octahedron and the already investigated dodecahedron. In these expandohedra, hexagons appear between faces as a consequence of the expansion. The expandable tetrahedron/cube expands from a regular tetrahedron/cube to a semi-regular truncated tetrahedron/octahedron. The expandable octahedron and icosahedron have more complicated motions, associated with the octagons and decagons that appear during expansion.

Further generalizations of the class of parent polyhedra are possible. One such takes the set of Archimedean polyhedra, which are composed of regular faces. The connecting triangle–rectangle–triangle links no longer all have the C_2 symmetry present in the Platonic models. With appropriate modification of the angles of the triangular plates, the expansion property can be retained, but the planarity of the 'empty faces' of the expanded structure may be lost. Other generalizations are also possible.

The following section treats an abstract version of the physical model, using symmetry and combinatorial arguments to understand some of the general features of the mechanisms of expandohedra.

2.4. Further degrees of freedoms

2.4.1. The mobility criterion

In Section 2.2, it was shown that the expandable dodecahedron is a finite mechanism and hence has at least 1 degree of freedom. However, the question arises whether there are additional degrees of freedom of the expandable dodecahedron. In kinematics, the Kutzbach measure gives a lower bound to the degrees of freedom (Hunt, 1978). Each separate rigid body has 6 degrees of freedom, and each revolute hinge connection has 1 degree of freedom, as at a hinge 5 degrees of freedom are lost, additionally the whole assembly has a rigid motion with 6 degrees of freedom that should be subtracted when counting the degrees of freedom of a hinge-connected mechanism. If the assembly is composed of b rigid bodies and h hinges, then the minimum number of degrees of freedom (the Kutzbach measure) f is

$$f = 6b - 5h - 6. \tag{9}$$

The dodecahedron has 12 prisms, 30 rectangles and 60 triangles, that is, $b = 102$. We can associate 10 hinges to each pentagonal face. Thus, $h = 120$. From (9), $f = 6$. This implies that the expandable dodecahedron has at least 6 degrees of freedom. It is not known whether each degree of freedom is finite, and other degrees of freedom, with associated states of self-stress may also be possible, by analogy with the extended Maxwell rule (Calladine, 1978). Section 3 will show that symmetry arguments can further elucidate the nature of these mechanisms; it will turn out that the 6 Kutzbach degrees of freedom are *additional* to the finite mechanism of Section 2.2.

2.4.2. Face mechanisms

The motion of the finite mechanism described in Section 2.2, involves, at a general point, all pentagonal faces simultaneously and symmetrically translating along, and rotating about, radial axes. There are however, special configurations: when the model is fully closed (Fig. 6, $\beta = \pm\pi/5$) the faces simultaneously translate, without rotation; when the model is fully open (Fig. 6, $\beta = 0$) the faces simultaneously rotate, without translation.

Experimentation with the fully closed physical model shows that, in addition to the finite mechanism that involves *simultaneous* translation of the faces, there are other, infinitesimal, mechanisms, where each face translates *independently*. Similarly, in the fully open state, there are infinitesimal mechanisms where the faces are able to rotate independently. The question arises: does each face have an independent infinitesimal mechanism at any stage of the expansion, involving coupled rotation and translation? The answer is not easy to determine experimentally for a general configuration, but the existence of these *face mechanisms* can be shown geometrically for the expandohedron based on the dodecahedron, as well as other cases.

Fig. 7 shows a linkage between faces of the expandohedron based on the dodecahedron; the two triangles and the rectangle featured in Fig. 2. Two features of the motion of this linkage will be shown: first, that with EF fixed, it is possible for B to move arbitrarily in the plane perpendicular to BE; second, that it is possible for the direction of line AB not to be altered by this arbitrary motion. These features will prove to be sufficient to show the existence of face mechanisms.

To show that the features of the motion of the linkage exist, we set up the following geometry. Consider unit vectors ef, ed, eb, bc, and ba that lie parallel to the lines EF, ED, EB, BC and BA, respectively. Also consider unit (infinitesimal) rotations R_{ef}, R_{ed} and R_{bc} about the lines EF, ED and BC, respectively. (We note that, as we are considering only infinitesimal motions, we can sum rotations in the same way that we sum vectors.) By the construction of the expandohedron, at any point in the expansion, BC and ED are parallel,

$$ed = bc, \tag{10}$$

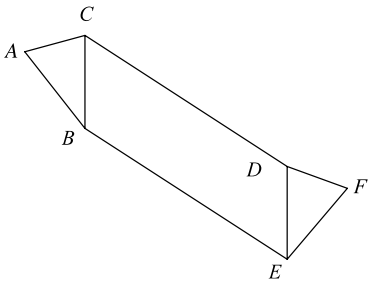

Fig. 7. The linkage between two faces.

whereas no two of EB, ED, EF are ever parallel,

$$eb \neq ed \neq ef \neq eb. \tag{11}$$

As ABC and DEF are parallel planes, it is possible to write

$$ab = \xi ed + \psi ef, \tag{12}$$

where scalars ξ and ψ depend on the current geometry, but $\psi \neq 0$, as this would imply that AB and BC were parallel.

The first feature of the motion of the linkage can now be shown straightforwardly. Consider line EF as fixed. By (11), rotations about EF and ED will allow B to move arbitrarily in the plane perpendicular to BE. In general, the rotation about the point E will be given by

$$R_E = xR_{ef} + yR_{ed}, \tag{13}$$

where x and y are arbitrary scalars.

The arbitrary R_E of (13) will in general lead to the rotation of the line AB so that it is no longer parallel with ab. To show the second feature, that AB may remain parallel to ab, requires that an additional rotation R_{bc} is able to correct for this. Consider a total rotation of line AB

$$R_{\text{tot}} = xR_{ef} + yR_{ed} + zR_{bc}. \tag{14}$$

If we choose $z = \xi x/\psi - y$, (14) becomes

$$R_{\text{tot}} = \frac{1}{\psi}\left[x(\xi R_{bc} + \psi R_{ef}) + \psi y(R_{ed} - R_{bc})\right]. \tag{15}$$

Substituting $R_{bc} = R_{ed}$, and $R_{ab} = \xi R_{ed} + \psi R_{ef}$, gives

$$R_{\text{tot}} = \frac{x}{\psi} R_{ab}. \tag{16}$$

Thus the total rotation of the line AB is about ab, and AB remains parallel with its initial direction.

Now consider a pentagonal prismatic face surrounded by five linkages. The features of the linkage, described above, imply the following, when all five linkages are considered together: (i) the distances between inner vertices connected by a linkage must be preserved; (ii) within this constraint, any motion that leaves the face parallel with its initial position is allowed. As the linkages around any face are arranged with C_5 symmetry, (i) and (ii) will always allow a local infinitesimal motion for each face independently, at a general configuration involving rotation about, and translation along, the local symmetry axis. Hence, the existence of face mechanisms has been shown for the expandohedron based on a dodecahedron.

The arguments above can be extended to show the existence of a face mechanism for almost any regular polygonal face of any expandohedron. The only restriction is that the face must not be parallel with an adjoining face, as (11) must remain true. With this restriction, a face mechanism must be possible for any triangular face; parallel motion of the face allows four local freedoms, while the length constraints between vertices only gives three constraints.

2.4.3. Edge mechanisms

In the fully open configuration, the triangular and rectangular plates constituting the connecting link between two face prisms become coplanar. In this special geometrical situation, an additional *edge mechanism* is possible, as shown in Fig. 8.

2.4.4. Geometry-based count of mechanisms

For the dodecahedron, the current section has found various mechanisms for a general configuration. Geometric reasoning showed the existence of a single breathing mechanism. Mobility counting showed that the number of mechanisms was at least six. Consideration of face mechanisms detected 12 degrees of

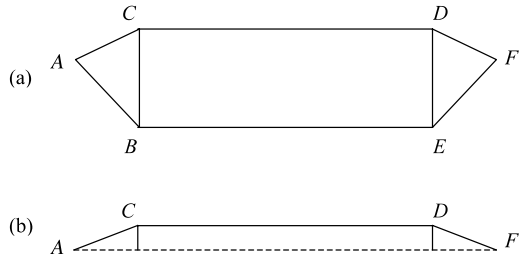

Fig. 8. The infinitesimal edge mechanism for the fully open configuration of an expandohedron. (a) Side view of starting configuration. (b) Displaced configuration viewed down the radius from the edge mid-point to the centre of the polyhedron. Points C and D can move infinitesimally in unison out of the plane containing the triangular and rectangular plates, without moving the points A, B, E and F that define the hinges to the prisms.

freedom. In the fully open configuration, there are also 30 edge mechanisms, that are independent of the 12 face mechanisms, and hence there are at least 42 degrees of freedom. The degree to which these various counts are independent will be established in the following sections.

3. Symmetry analysis

3.1. The mobility of an expandohedron

In the language of polyhedra and related combinatorics, the general construction can be described as follows. Call the parent polyhedron P. The expandohedron E is constructed from the elements of P as shown schematically in Fig. 9. First, the faces of P are separated: E contains a distinct rigid prism for each face of P, the same in size and shape as the original (Fig. 9(a)). Each edge of P is thereby doubled, with the edge ab, that was common to two faces now replaced by edges $a'b'$ and $a''b''$ of the separated faces (Fig. 9(b)). The rigid face prisms are now connected by a triple of rigid plates, hinged at a', a''', b''', b'' (Fig. 9(c)), one such assembly for each original edge. The choice of hinge points for the connecting triple (i.e. the choice to connect $a' \ldots b''$, or $a'' \ldots b'$) is made cyclically on some starting face, and then propagated consistently over the whole set of face prisms.

By construction, E consists of $f + 3e$ rigid bodies and $4e$ hinges, where f and e are the numbers of faces and edges of P, which are related to v, the number of vertices of P, by the Euler relation for spherical polyhedra, $v + f = e + 2$. It is also useful to define a contact polyhedron C, derived from E by taking every rigid body in E as a *vertex* of C, and every linkage between rigid bodies (in this case every hinge) as an *edge* of C. C has $4e$ edges, and $f + 3e$ vertices, of which $3e$ are divalent. Strictly speaking, as it has divalent vertices, C is a *spherical map* rather than a polyhedron.

The construction of E preserves all proper (rotational) symmetries that were present in P, but removes any improper (reflection, rotation–reflection, inversion) symmetries. Hence, E is a chiral object. At all positions short of full opening, E has a maximal symmetry defined by the full rotational subgroup of the point group of P itself. When E is fully opened, each connecting triple will be linear and can be taken as a composite edge of the leapfrog of P. If P is achiral, E then regains the full symmetry of P and continuation of the finite 'opening' motion from this achiral configuration will start to close the structure along a mirror-image path.

It is useful to establish some notation for the subsequent discussion of mobility and symmetry. In $G(E)$, the point group of E, Γ_T and Γ_R are the three-dimensional representations of translations along, and rotations about the Cartesian axes. In the same group, $\Gamma_\sigma(x, X)$ is the permutation representation of struc-

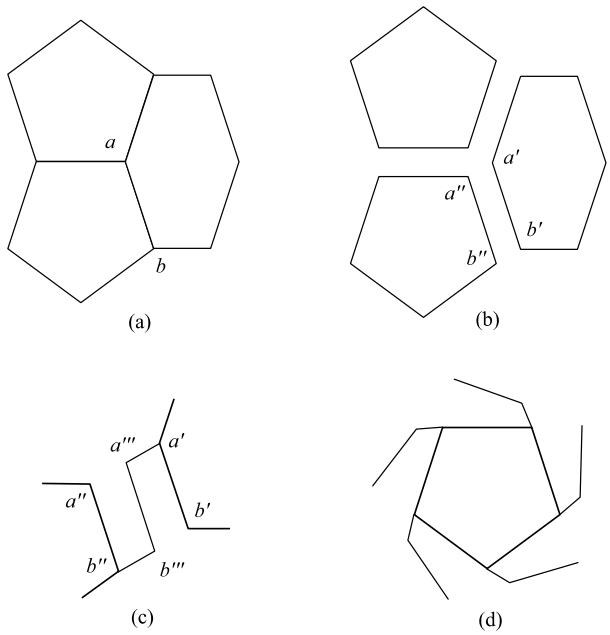

Fig. 9. (a) The original polyhedron has an edge *ab* common to two faces; (b) the expandohedron has two copies of *ab*; (c) the edge *ab* is replaced by a triple of rigid bodies, hinged at a', a''', b''', b''; (d) a consistent choice of connecting triples is made cyclically on one face and then propagated over P to produce the full structure of the expandohedron E.

tural components of x of X, with characters defined by the number of x that remain *un*shifted under a given operation, and $\Gamma_{\parallel}(e,X)$ and $\Gamma_{\perp}(e,X)$, represent sets of vector respectively along and across edges of X, all orthogonal to the radius vector of the edge midpoint. As the point group that is being used, $G(E)$, is always that of a chiral polyhedron, the distinction between Γ_T and Γ_R and between $\parallel$ and $\perp$ edge vectors is lost. Likewise, the pseudo-scalar representation Γ_{ε}, which is defined to have character +1 under proper and −1 under improper operations, reduces to the totally symmetric representation, Γ_0, in these cases. For the chiral polyhedra and assemblies under study here, we will use

$$\Gamma_{\rightarrow}(e,X) \equiv \Gamma_{\parallel}(e,X) \equiv \Gamma_{\perp}(e,X), \quad \Gamma_{xyz} \equiv \Gamma_T \equiv \Gamma_R, \quad \Gamma_0 \equiv \Gamma_{\varepsilon}. \tag{17}$$

The symmetry version of the general mobility criterion for assemblies of rigid bodies (Guest and Fowler, 2003) is

$$\Gamma(\text{freedom}) - \Gamma(\text{constraints}) = \Gamma(m) - \Gamma(s). \tag{18}$$

Here, Γ(freedom) is the representation of the $6N-6$ degrees of freedom of the set of N unlinked rigid bodies, Γ(constraints) is the representation of those degrees of freedom removed by the constraints imposed by the links between the rigid bodies, and $\Gamma(m)$ and $\Gamma(s)$ are the representations of the set of mechanisms and the states of self-stress of the linked assembly, respectively.

The relative freedoms span the translations and rotations of the N bodies, *minus* the overall rigid-body motions of the assembly. Thus

$$\Gamma(\text{freedom}) = (\Gamma_T + \Gamma_R) \times \Gamma(\text{bodies}) - \Gamma_T - \Gamma_R, \tag{19}$$

where Γ(bodies) is the permutation representation of the bodies. In the present case, the body centres comprise: one for each face of the parent polyhedra, one at the midpoint of each old edge of the parent

polyhedron, and a pair symmetrically disposed about that midpoint. In terms of the faces and edges of P, therefore,

$$\Gamma(\text{bodies}) = \Gamma_\sigma(f,P) + 2\Gamma_\sigma(e,P) + \Gamma_\parallel(e,P), \tag{20}$$

where the vector representation $\Gamma_\parallel(e,P)$ arises from counting the symmetrical pairs of bodies as sums of in-phase ($\Gamma_\sigma(e,P)$) and out-of-phase ($\Gamma_\parallel(e,P)$) combinations on each edge. All representations are to be understood as representations in $G(E)$, rather than the full group $G(P)$, even when they refer to elements of P, and so, for example, $\Gamma_\parallel(e,P)$ can be replaced by $\Gamma_\rightarrow(e,P)$ in (20).

The form of Γ(constraints) depends on the mode of linkage. Rigid gluing would remove freedoms corresponding to the relative rotation and translation of each glued pair, and hence contribute constraints spanning $\Gamma_\parallel(e,C) \times (\Gamma_T + \Gamma_R) \equiv 2\Gamma_\rightarrow(e,C) \times \Gamma_{xyz}$; replacement of rigid glue by the revolute hinges used in E restores freedoms spanning $\Gamma_\perp(e,C) \equiv \Gamma_\rightarrow(e,C)$. By construction, the contact polyhedron C corresponding to E, since both are chiral, has

$$\Gamma_\rightarrow(e,C) = 2\Gamma_\rightarrow(e,P) + 2\Gamma_\sigma(e,P), \tag{21}$$

and

$$\Gamma(\text{constraints}) = \{2\Gamma_\rightarrow(e,P) + 2\Gamma_\sigma(e,P)\} \times \{\Gamma_{xyz} - \Gamma_0\}. \tag{22}$$

From which, combining (20)–(22),

$$\Gamma(m) - \Gamma(s) = 2\{\Gamma_\sigma(f,P) - \Gamma_\rightarrow(e,P)\} \times \Gamma_{xyz} + 2\{\Gamma_\sigma(e,P) + \Gamma_\rightarrow(e,P)\} - 2\Gamma_{xyz}. \tag{23}$$

The character of (23) under the identity recovers the count of the excess of mechanisms over states of self-stress i.e. $m - s = 4e - 6v + 6$.

An alternative form of (23), also valid for all E, can be derived. As we are working in the group $G(E)$, which contains only proper operations, the symmetry extension of the Euler theorem (Ceulemans and Fowler, 1991) reduces to

$$\Gamma_\sigma(f,P) = \Gamma_\rightarrow(e,P) + 2\Gamma_0 - \Gamma_\sigma(v,P), \tag{24}$$

from which

$$\Gamma(m) - \Gamma(s) = 2\{\Gamma_\sigma(e,P) + \Gamma_\rightarrow(e,P) - \Gamma_\sigma(v,P) \times \Gamma_{xyz} + \Gamma_{xyz}\}. \tag{25}$$

The RHS of (23) and (25) can be calculated directly for any given parent P. For the five Platonic and 13 Archimedean solids, the results are shown in Table 1. The fact that all trivalent polyhedra in the table have $m - s = 6$, and that these extra mechanisms transform as $2\Gamma_{xyz}$ is not accidental, as it can be proved that $\Gamma(m) - \Gamma(s)$ is equal to $2\Gamma_{xyz}$ for all E derived from trivalent parents.

One proof proceeds as follows. For trivalent parents P, a general property of the vertex representation for trivalent polyhedra (Ceulemans and Fowler, 1991) reduces in $G(E)$ to

$$\Gamma_\sigma(v,P) \times \Gamma_{xyz} = \Gamma_\sigma(e,P) + \Gamma_\rightarrow(e,P), \tag{26}$$

and so

$$E(P), P \text{ trivalent}: \quad \Gamma(m) - \Gamma(s) = 2\Gamma_{xyz}. \tag{27}$$

A simpler proof is by characters. Let $\chi_\sigma(R)$ and $\chi_\rightarrow(R)$ be the characters under operation R of $\Gamma_\sigma(e,P)$ and $\Gamma_\rightarrow(e,P)$, respectively. In the chiral group $G(E)$, an edge of P either lies on no non-trivial symmetry element or is bisected by a C_2 axis. The contribution of any one edge to $\chi_\sigma(R) + \chi_\rightarrow(R)$ is $(+1) + (-1)$ for such a C_2 operation, $(+1) + (+1)$ for the identity, and $(0) + (0)$ otherwise. Thus, $\Gamma_\sigma(e,P) + \Gamma_\rightarrow(e,P)$ has character $2e$ under the identity and zero otherwise. Similarly, a vertex of P either lies on a C_3 axis or is on no non-trivial

Table 1
Mobility of expandohedra based on Platonic and Archimedean polyhedra of degree d, as predicted by the symmetry-extended version of the mobility criterion. m and s are the counts of mechanisms and states of self-stress, respectively, and Γ is a representation in the point group $G(E)$ of the chiral expandohedral structure

P	$\Gamma(P)$	$\Gamma(E)$	d	$m-s$	Γ_{xyz}	$\Gamma(m)-\Gamma(s)$
Tetrahedron	T_d	T	3	6	T	$2T$
Octahedron	O_h	O	4	18	T_1	$2A_2+2E+2T_1+2T_2$
Cube	O_h	O	3	6	T_1	$2T_1$
Icosahedron	I_h	I	5	54	T_1	$2T_1+4T_2+4G+4H$
Dodecahedron	I_h	I	3	6	T_1	$2T_1$
Truncated tetrahedron	T_d	T	3	6	T	$2T$
Truncated cube	O_h	O	3	6	T_1	$2T_1$
Truncated octahedron	O_h	O	3	6	T_1	$2T_1$
Truncated dodecahedron	I_h	I	3	6	T_1	$2T_1$
Truncated icosahedron	I_h	I	3	6	T_1	$2T_1$
Cuboctahedron	O_h	O	4	30	T_1	$2A_1+2E+4T_1+4T_2$
Icosidodecahedron	I_h	I	4	66	T_1	$2A+4T_1+2T_2+4G+6H$
Rhombicuboctahedron	O_h	O	4	54	T_1	$2A_1+2A_2+4E+8T_1+6T_2$
Rhombicosidodecahedron	I_h	I	4	126	T_1	$2A+8T_1+6T_2+8G+10H$
Truncated cuboctahedron	O_h	O	3	6	T_1	$2T_1$
Truncated icosidodecahedron	I_h	I	3	6	T_1	$2T_1$
Snub cube	O	O	5	102	T_1	$4A_1+4A_2+8E+14T_1+12T_2$
Snub dodecahedron	I	I	5	246	T_1	$4A+14T_1+12T_2+16G+20H$

symmetry element of $G(E)$. As $\chi_{xyz}(C_3)=0$, the vertex representation $\Gamma_\sigma(v,P)\times\Gamma_{xyz}$ for trivalent P has character $3v$ under the identity, and zero otherwise. The vertex and edge terms on the RHS of (25) therefore cancel out, recovering (27).

This explains the results for the trivalent Platonic polyhedra: for *any* trivalent parent polyhedron, the excess of mechanisms over states of self-stress is six, is independent of the details of P, and spans the symmetry $2\Gamma_{xyz}$. In particular, this implies that the leapfrog expandohedron derived from any one of the infinite class of fullerene polyhedra has six mechanisms that transform as translations, or equivalently rotations.

The argument can be extended to show that an expandohedron E based on *any* parent polyhedron P has *at least* these mechanisms. Consider a decoration of the edges of P in which two marks are placed symmetrically on each edge, one close to each end vertex. The permutation representation of the set of marker points is then $\Gamma_\sigma(e,P)+\Gamma_\rightarrow(e,P)$. However, the marks also form cycles around the vertices, with a set of d points surrounding a vertex of degree d, and so their permutation representation contains *at least* the symmetries of a scalar and two tangential vector combinations at each vertex, i.e. $\Gamma_\sigma(v,P)\times\Gamma_{xyz}$. The composite representation $\Gamma_\sigma(e,P)+\Gamma_\rightarrow(e,P)-\Gamma_\sigma(v,P)\times\Gamma_{xyz}$ is therefore a reducible representation with non-negative contributions from all the irreducible representations of $G(E)$, and hence it is possible to state, with a slight abuse of set-theory notation that

$$\text{all parent } P: \quad \{\Gamma(m)-\Gamma(s)\}\supset 2\Gamma_{xyz}, \tag{28}$$

where $\supset$ is used here, and subsequently, to denote that $\Gamma(m)-\Gamma(s)$ must contain at least $2\Gamma_{xyz}$. For non-trivalent polyhedra P, the RHS of (25) is no longer independent of P, but can always be written as $2\Gamma_{xyz}$ *plus* a function of the vertices of P.

The results for the mobility of expandohedra based on all the Platonic and Archimedean polyhedra are given in Table 1.

3.2. Symmetry of face mechanisms

It was shown in Section 2.4.2 that there was a local infinitesimal mechanism associated with each of the prisms of an expandohedron; if P has f faces, there will be f such mechanisms. This set of mechanisms will transform under the operations of $G(E)$ in the same way as the faces of P, and hence the character of this set of mechanisms will be $\Gamma_\sigma(f,P)$. It is thus possible to state that

$$\Gamma(m) \supset \Gamma_\sigma(f,P), \tag{29}$$

i.e. that the representation spanned by the mechanisms of E *includes* that of the faces of P. It is, of course, not possible to say that $\Gamma_\sigma(f,P)$ is the complete set of infinitesimal mechanisms.

3.3. Predictions for mechanisms and states of self-stress

The results from the two previous sections can be combined to deduce a minimal set of mechanisms and states of self-stress that must be present. For the case when P is one of the trivalent Euler polyhedra, a remarkably simple result is found by combining (27) and (29),

$$E(P), P \text{ trivalent}: \quad \Gamma(m) \supset \Gamma_\sigma(f,P) \cup \{\Gamma_{xyz} + \Gamma_{xyz}\}. \tag{30}$$

For the Platonic solids, however, the permutation representation for the faces is that of a single orbit, and each happens to contain exactly one copy of Γ_{xyz}, (all orbits of more than four objects generate *at least one* copy of Γ_{xyz}, but the larger orbits contain two or more copies—it so happens that these larger orbits correspond to Archimedean rather than Platonic solids) and hence

$$E(P), P \text{ trivalent, Platonic}: \quad \Gamma(m) \supset \Gamma_\sigma(f,P) + \Gamma_{xyz}, \tag{31}$$

and, as for this case $\Gamma(m) - \Gamma(s) = 2\Gamma_{xyz}$,

$$E(P), P \text{ trivalent, Platonic}: \quad \Gamma(s) \supset \Gamma_\sigma(f,P) - \Gamma_{xyz}. \tag{32}$$

Section 4 will show that the RHS of (31) and (32) are in fact the complete sets of mechanisms and states of self-stress for the expandohedra based on trivalent Platonic solids.

3.4. Predictions for m and s at the fully open configuration

It was shown in Section 2.4.3 that when the set of plates constituting a link between prisms becomes planar, an extra edge mechanism is introduced. For the expandohedra derived from Platonic polyhedral parents, all links will become planar simultaneously in the fully open configuration. The symmetry spanned by the e edge mechanisms is that of a set of translations across the edges of E, or equivalently along the edges of P, and hence is equal to $\Gamma_{\rightarrow}(e,P)$ in $G(E)$, as defined in (17).

It is thus possible to state that the set of mechanisms of E at the fully open configuration includes $\Gamma_{\rightarrow}(e,P)$

$$E(P), P \text{ trivalent, open}: \quad \Gamma(m) \supset \Gamma_{\rightarrow}(e,P). \tag{33}$$

Combining (33) with (30) then gives, for the total set of mechanisms

$$E(P), P \text{ trivalent, open}: \quad \Gamma(m) \supset \{\Gamma_\sigma(f,P) + \Gamma_{\rightarrow}(e,P)\} \cup \{\Gamma_{xyz} + \Gamma_{xyz}\}, \tag{34}$$

and, as $\Gamma_\sigma(f,P) \supset \Gamma_{xyz}$, and $\Gamma_{\rightarrow}(e,P) \supset \Gamma_{xyz}$, for the trivalent Platonic parents in the symmetry group $G(E)$, the minimal set of mechanisms in the fully open configuration is

$$E(P), P \text{ trivalent, open}: \quad \Gamma(m) \supset \{\Gamma_\sigma(f,P) + \Gamma_{\rightarrow}(e,P)\}, \tag{35}$$

which is of dimension $f + e = 2v + 2$.

Note that at the fully open configuration the structure actually has the symmetry $G(P)$, which, for achiral P includes $G(E)$ as a rotational subgroup.

4. Numerical modelling

4.1. Description of the model

This section will describe a numerical model of the expandohedra based on the dodecahedron, tetrahedron and the cube that confirms the analysis in the previous sections. It shows that in general configurations there are no additional infinitesimal mechanisms beyond those predicted by (31). In the fully open configuration there are no additional infinitesimal mechanisms beyond those predicted by (35).

A numerical model could be set up most straightforwardly using a simple bar-and-joint assembly (see e.g. Calladine, 1978; Pellegrino, 1993). Here the problem is more difficult because it is necessary to model a series of rigid bodies, while at the same time preserving the symmetry of the assembly for a later symmetry-adapted analysis. Hence, the model incorporates additional vectors and constraints chosen to describe the planarity of connecting plates and the geometry of the triangular plates hinged to the prisms. Similar extensions of bar and joint models are described in Guest and Pellegrino (1994), and Kovács et al. (1997).

Expandohedra consist of three different elements, prisms, rectangular plates, and triangular plates, hinged together by revolute hinges. The different elements were modelled as follows:

(i) The model for an n-gonal prism is shown in Fig. 10(a) for the particular case of $n = 3$. It consists of $(n + 2)$ nodes, and $3n$ bars, arranged to form an n-gonal bipyramid, and is statically and kinematically determinate. The axial vertices of the bipyramids define vectors **u** perpendicular to the n-gonal faces of the prism. These vectors are used to define the hinge constraints at the connection to the triangular plates.

(ii) The model of the rectangular plate is shown in Fig. 10(b). It consists of a bar linking two existing nodes, and a unit vector **v**, perpendicular to the bar, that is defined to lie in the plane of the plate.

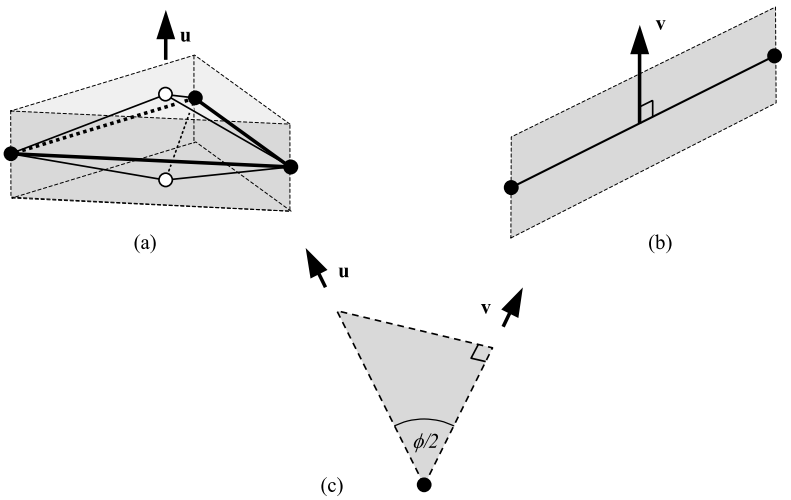

Fig. 10. Modified bar and joint models of: (a) face prisms; (b) rectangular plates; (c) triangular plates.

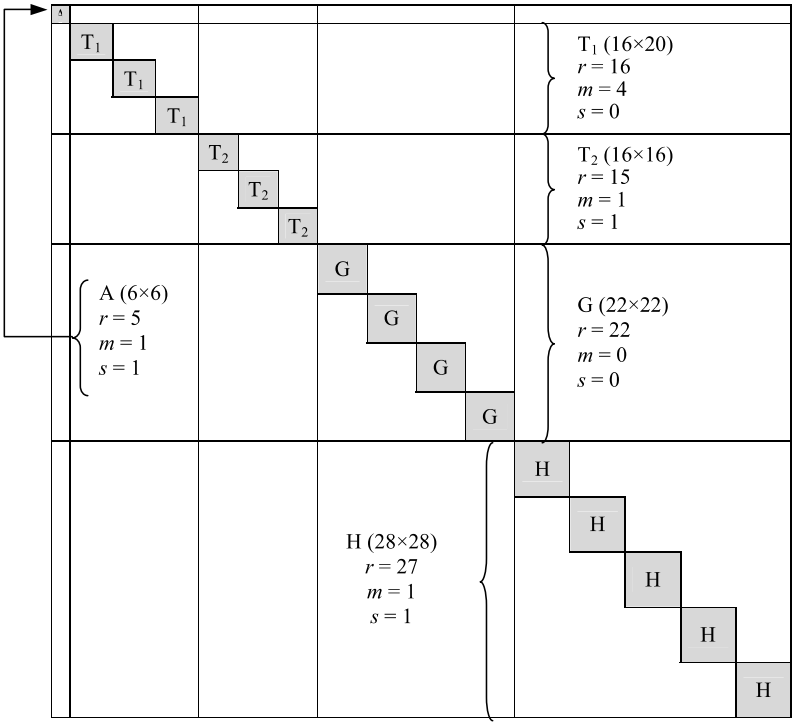

Fig. 11. Structure of the compatibility matrix **C** for the expandable dodecahedron. Each symmetry block is labelled by irreducible representation, size, rank (r), number of mechanisms (m), and states of self-stress (s).

(iii) The model of the triangular plate is shown in Fig. 10(c). It consists only of a constraint that the angle between the two hinges on the plate is preserved.

4.2. Symmetry-adapted analysis

The model described in Section 4.1 allows a *compatibility matrix*, **C**, to be defined and used to find possible infinitesimal mechanisms of the structure (the nullspace of **C**), and any overconstraint, corresponding to states of self-stress (the left-nullspace of **C**). See e.g. Pellegrino and Calladine (1986) for more details. When the expandohedron is highly symmetric, it is instructive to perform the decomposition of **C** in a *symmetry-adapted* manner, as described by Kangwai and Guest (2000). The constraints and freedoms are written using a symmetry-adapted coordinate system, and this leads to the matrix **C** taking on a block-diagonal form, with each block corresponding to a component of an irreducible representation of $G(E)$.

4.3. Results

4.3.1. The expandable dodecahedron

The results presented here were calculated at two configurations: the fully closed configuration, as representative of a general point in the expansion, and the fully open configuration, when additional rank-deficiency appears in the matrix **C**.

For the dodecahedron, each of the prisms has $n = 5$, hence 7 nodes, and 21 freedoms, and 15 bars forming 15 constraints. For the entire structure, there are: 12 prisms, giving 252 freedoms and 180 con-

Table 2
Results of symmetry-adapted matrix analysis for the expandohedra based on the three trivalent Platonic polyhedra in both the closed and fully open configurations

Parent polyhedron $\Gamma_\sigma(f,P)$, $\Gamma_\rightarrow(e,P)$	Block	Block size	General configuration		Fully open configuration	
			Number of states of self-stress	Number of mechanisms + rigid-body motions	Number of states of self-stress	Number of mechanisms + rigid-body motions
Tetrahedron						
$A+T$,	A	6×6	1	1	1	1
$2T$	E	12×12	2×0	2×0	2×0	2×0
	T	16×20	3×0	3×4	3×1	3×5
	Total	66×78	1	13	4	16
Cube						
A_1+E+T_1,	A_1	6×6	1	1	1	1
$A_2+E+2T_1+T_2$	A_2	5×5	0	0	1	1
	E	11×11	2×1	2×1	2×2	2×2
	T_1	16×20	3×0	3×4	3×1	3×5
	T_2	17×17	3×0	3×0	3×1	3×1
	Total	132×144	3	15	12	24
Dodecahedron						
$A+T_1+T_2+H$,	A	6×6	1	1	1	1
$2T_1+2T_2+2G+2H$	T_1	16×20	3×0	3×4	3×1	3×5
	T_2	16×16	3×1	3×1	3×3	3×3
	G	22×22	4×0	4×0	4×2	4×2
	H	28×28	5×1	5×1	5×3	5×3
	Total	330×342	9	21	36	48

straints; 30 rectangular plates, giving 90 freedoms, and 90 constraints; 60 triangular plates, giving 60 constraints. Thus, in total, there are 342 freedoms, and 330 constraints. Altogether, there are 12 more freedoms than constraints, and thus there are 12 independent mechanisms by which the structure can move. However, we know that 6 of these will be rigid-body motions, leaving 6 internal mechanisms, in agreement with the mobility count of Section 2.4.1.

Singular-value decomposition of the matrix **C** showed a rank-deficiency of 9. This gives 21 mechanisms, and 9 states of self-stress. Block-diagonalization of **C** (see Fig. 11) shows that of these mechanisms, there are 15 that are not rigid body motions and are distributed amongst the different irreducible representations of the icosahedral group as follows:

$$\Gamma(m) = A + 2T_1 + T_2 + H. \tag{36}$$

This is exactly as predicted from the sum of the face representation of the dodecahedron,

$$\Gamma_\sigma(f,E) = A + T_1 + T_2 + H, \tag{37}$$

and the translational representation $\Gamma_{xyz} = T_1$.

In the fully open configuration of the expandable dodecahedron, the internal mechanisms span

$$\Gamma(m) = A + 3T_1 + 3T_2 + 2G + 3H \tag{38}$$

in the group $G(E) = I$. This again is exactly as predicted; (38) is from the sum of the face representation of the dodecahedron (37) and the representation of edge vectors

$$\Gamma_{\rightarrow}(e,E) = 2T_1 + 2T_2 + 2G + 2H. \tag{39}$$

4.3.2. Trivalent Platonic expandohedra: summary

Table 2 summarises the matrix analysis for the three expandohedra based on trivalent Platonic parents. In both general and fully open configuration, the numbers and symmetries of the mechanisms and the states of self-stress are in full agreement with the predictions embodied in the expressions (31), (32) and (35). Explicitly, the symmetry expressions give: for the tetrahedron $\Gamma(m)$ is $A + 2T$ in the general configuration, and $A + 3T$ in the fully open configuration; for the cube $\Gamma(m)$ is $A_1 + E + 2T_1$ in the general configuration, and $A_1 + A_2 + 2E + 3T_1 + T_2$ in the fully open configuration. For each of the three expandohedra, the mechanisms in the general configuration are accounted for by the face mechanisms plus a constant set of three mechanisms with the symmetry of the translations. In the fully open configurations, the face and edge mechanisms account exactly for the computed results.

5. Conclusions

This paper has used a combination of geometry, symmetry and numerics to provide a detailed understanding of the kinematics of expandohedra; each of these techniques makes an essential contribution to the paper.

The original expandohedron (Kovács and Tarnai, 2000) was designed to exhibit a finite breathing motion as a physical model of the experimentally observed swelling of viruses. This key feature escapes elementary counting of mobility, but is revealed by the symmetry analysis to be a totally symmetric combination of face mechanisms.

The numerical calculations in Section 4 detect all possible infinitesimal motions, and in particular finds the expected totally symmetric breathing mechanism. However, these numerical methods alone cannot establish the finite character of the breathing motion because of the presence of states of self-stress. In particular the method described by Kangwai and Guest (1999) is not applicable, because an equisymmetric state of self-stress has the potential to stiffen the breathing mechanism. However, the geometric arguments of Section 2 do establish the breathing motion's finite character. Experimentation suggests that the other mechanisms detected are not finite; any attempt to displace the physical models in these directions apparently leads to locking of these mechanisms.

Finally, it should be noted that the experimental observations on viruses show a more complex double link between adjacent morphological units (Speir et al., 1995); these links pair vertices and edge mid-points on adjacent prisms. The expandable dodecahedron can be adapted to reproduce this feature, but the breathing motion then requires the links to have an additional twisting degree of freedom. For example, four plates connected by revolute hinges, where the central hinge is perpendicular to adjacent hinges, could form the links. This new expandable dodecahedron behaves similarly to the single-link version, with a smaller range of expansion. Many other generalizations are also possible.

Acknowledgements

The research reported here was done within the framework of the Hungarian–British Intergovernmental Science and Technology Cooperation Programme with the support of OMFB and the British Council, TéT Grant No. GB-15/98. Partial support by OTKA Grant No. T031931 and FKFP Grant No. 0177/2001 is also gratefully acknowledged. SDG acknowledges support from the Leverhulme Trust.

References

Calladine, C.R., 1978. Buckminster Fuller's "Tensegrity" structures and Clerk Maxwell's rules for the construction of stiff frames. International Journal of Solids and Structures 14, 161–172.

Ceulemans, A., Fowler, P.W., 1991. Extension of Euler's theorem to the symmetry properties of polyhedra. Nature 353, 52–54.

Fowler, P.W., Steer, J.I., 1987. The leapfrog principle: a rule for electron counts of carbon clusters. Journal of the Chemical Society Chemical Communications, 1403–1405.

Fowler, P.W., Guest, S.D., 2000. A symmetry extension of Maxwell's rule for the rigidity of frames. International Journal of Solids and Structures 37, 1793–1804.

Fuller, R.B., 1975. Synergetics: Exploration in the Geometry of Thinking. Macmillan, New York.

Guest, S.D., Fowler, P.W., 2003. A symmetry-extended mobility rule. Submitted to Mechanism and Machine Theory.

Guest, S.D., Pellegrino, S., 1994. The folding of triangulated cylinders. Part II: The folding process. ASME Journal of Applied Mechanics 61, 777–783.

Hoberman, C., 1991. Radial Expansion/Retraction Truss Structures. United States Patent, Patent no.: 5,024,031.

Hunt, K.H., 1978. Kinematic Geometry of Mechanisms. Clarendon Press, Oxford.

Kangwai, R.D., Guest, S.D., 1999. Detection of finite mechanisms in symmetric structures. International Journal of Solids and Structures 36, 5507–5527.

Kangwai, R.D., Guest, S.D., 2000. Symmetry-adapted equilibrium matrices. International Journal of Solids and Structures 37, 1525–1548.

Kollár, L., Hegedűs, I., 1985. Analysis and Design of Space Frames by the Continuum Method. Akadémiai Kiadó, Budapest/Elsevier Science Pub, Amsterdam. p. 146.

Kovács, F., Hegedűs, I., Tarnai, T., 1997. Movable pairs of regular polyhedra. In: Proceedings of International Colloquium on Structural Morphology, Nottingham, pp. 123–129.

Kovács, F., Tarnai, T., 2000. An expandable dodecahedron. In: Bridge Between Civil Engineering and Architecture, Proceedings of the 4th International Colloquium on Structural Morphology. Delft University of Technology, Delft, pp. 227–234.

Pellegrino, S., 1993. Structural computations with the singular-value decomposition of the equilibrium matrix. International Journal of Solids and Structures 30, 3025–3035.

Pellegrino, S., Calladine, C.R., 1986. Matrix analysis of statically and kinematically indeterminate frameworks. International Journal of Solids and Structures 22, 409–428.

Seffen, K.A., Pellegrino, S., Parks, G.T., 1999. Deployment of a panel by tape-spring hinges. In: Proceedings of the IUTAM-IASS Symposium on Deployable Structures: Theory and Applications, 6–9 September 1998. Kluwer, Cambridge, UK.

Speir, J.A., Munshi, S., Wang, G., Baker, T.S., Johnson, J.E., 1995. Structures of the native and swollen forms of cowpea chlorotic mottle virus determined by X-ray crystallography and cryo-electron microscopy. Structure 3, 63–78.

Verheyen, H.F., 1989. The complete set of jitterbug transformers and the analysis of their motion. Computers and Mathematics with Applications 17, 203–250.